ICAS Paper No. 70-61

AERODYNAMIC ENERGY EXCHANGERS FOR HYBRID AIRBREATHING-ROCKET PROPULSION SYSTEMS

by
Felix Berner and Max Hermann
Consulting Engineers
Federal Aircraft Factory, Research Department
Emmen, Switzerland

The Seventh Congress of the International Council of the Aeronautical Sciences

CONSIGLIO NAZIONALE DELLE RICERCHE, ROMA, ITALY / SEPTEMBER 14-18, 1970

Price: 400 Lire

AERODYNAMIC ENERGY EXCHANGERS FOR HYBRID AIRBREATHING-ROCKET PROPULSION SYSTEMS*

F. Berner and M. Hermann
Consulting Engineers
Lucerne, Switzerland

Abstract

New methods of direct exchange of mechanical energy between flows have been investigated theoretically and experimentally. These methods are of interest for propulsion systems of the ramjet type incorporating a rocket motor as a source of high energy gas. The investigated concepts differ from the ejector in that the energy exchange is based not only on shear stresses but also on moving pressure fields.

Results of the analytical and experimental investigation are presented and are compared with the corresponding data of ejectors operating with the same driving and driven media.

I. Introduction

During the last few years considerable interest has developed for jet propulsion systems which have characteristics intermediate to those of pure chemical rockets on the one hand and aviation gas turbines on the other hand. The reason for this interest are the very low specific impulse of chemical rockets which is inadequate for many missions, and the modest thrust-to-weight ratio of turbo-jet engines which makes these powerplants unattractive for many boost missions, particularly at launch and at flight speeds where they can swallow only a fraction of the air which they intersect.

In principle it would be possible to close the gap in the propulsion spectrum between pure airbreathers and chemical rockets either by modifying aviation gas turbines with the aim of increasing their thrust-to-weight ratio and extending the speed range within which they can operate, or by adding to pure chemical rockets certain components which enable them to use some of the surrounding atmosphere as momentum medium and as oxidizer. Because gasturbines are very complex machines while chemical rockets are among the simplest propulsion devices known, interest has focused primarly on measures involving the addition of air-processing components to chemical rockets with the aim of increasing their specific impulse at the expence of their very high thrust-to-weight ratio.

A relatively simple scheme of combining air with rocket gases is realized in the so-called shrouded rocket: The scooped air is conducted to the divergent portion of the rocket nozzle and is introduced circumferentially with a radial velocity component. The rocket gases being rather strongly fuel-rich, some of the excess fuel is burnt upon contact with the air's oxygen. This air-augmentation scheme results in relatively small thrust increases because the mixing and secondary combustion processes are limited by the fact that they take place in a region where the rocket gases have already attained supersonic velocities and where the distance from the engine (i.e., nozzle) exit is short, so that the residence time of the interacting media in the engine is very short.

A larger degree of thrust augmentation is possible if the interaction of rocket gas and aspirated or scooped air takes place at relatively low flow velocities and, in particular, when secondary combustion takes place at subsonic velocities. Here, however, the components for inducting the air, for achieving an energy exchange between rocket gas and air, and their mixing and for secondary combustion become rather large and the rocket motor(s) quite often are buried within the resultant engine. In fact, engines of this type can no longer be classified as rocket engines but represent a new class of propulsion systems: Hybrid airbreathing-rocket propulsion systems. Most of these engines perform in the hybrid mode only at low and intermediate flight speeds and are operated as ramjet engines at flight Mach numbers above 2. Also their appearance is more or less that of ramjets. Differences between such hybrid engines and ramjets are in the internal configuration. Hybrid engines possess in addition to the ramjet components one or several rocket-type gas generators as an energy source and means for the transfer of mechanical energy and momentum from the rocket gas to the inducted air and for the mixing of the rocket gas with the air. The thermodynamic cycle of hybrid engines differs from that of turbojet engines with afterburners in that the turbomachinery and primary combustion chamber are replaced by the gas generator and by the energy transfer means. Rocket type gas generators are perhaps the lightest possible energy sources. A similar statement cannot be made for all energy exchangers. It should be noted, however, that a combination energy source/energy exchanger must, in general, offer a marked weight advantage over the combination compressor-primary combustion chamber-turbine if the less efficient hybrid engine shall successfully compete with the turbojet engine. For certain missions it is also of interest to find an optimum tradeoff between the efficiency and the weight

*) This work was carried out at the Federal Aircraft Factory, Research Dept., Emmen, Switzerland

of the energy exchanger.

II. Energy Exchange Methods for Hybrid Engines

As mentioned above, there are two tasks to be performed downstream of the primary energy source of hybrid engines and upstream of the position where secondary combustion takes place: Mechanical energy or momentum must be transferred between the rocket gas jet (primary flow) and the air (secondary flow) and the two media must be mixed. There are several ways for achieving these functions. The momentum transfer can be direct or indirect and it can proceed before mixing takes place or it can occur concurrently with the mixing process.

A method of indirect mechanical energy exchange between flows involves a turbine-turbocompressor combination (Fig. 1 a).

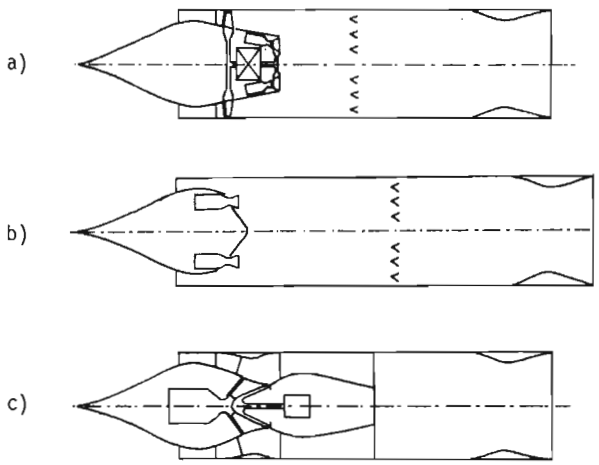

Fig. 1. Schematic drawing of some hybrid air-breathing-rocket propulsion systems (a) Turborocket engine, (b) ejector-ramjet engine, (c) propulsion system with aerodynamic energy exchanger.

This method is realized in turbo-rocket engines. A turbine extracts energy from the gas flow provided by the gas generator and then drives a turbocompressor which imparts energy to the inducted air. As a result of this energy exchange the momentum of the primary and secondary flows downstream of turbine and compressor is nearly the same. Consequently no large energy dissipation occurs during the subsequent mixing process. In fact, the overall energy exchange efficiency (taking mixing into account) is not much lower than the product of turbine and compressor efficiency and can approach about 50 % even if the turbine is of the partial admission type.

On the other hand this energy transfer scheme requires rather heavy equipment, particularly if a large reduction of the rotational speed between turbine and compressor must be achieved.

A direct momentum exchange is achieved in ejectors whereby it occurs simultaneously with the mixing of the fluids. Propulsion systems utilizing this component usually are called ejector-ramjets or ducted rockets (see Fig. 1 b). Ejectors are very simple devices: Besides the rocket-type gas generators they merely consist of a simple duct (mixing tube). However, their efficiency is rather low, particularly for secondary fluid density-to-primary fluid density ratios typical for ducted rockets at take-off. The low efficiency is due to the fact that the energy exchange results from viscous stresses rather than the action of moving pressure fields as in turbomachines.

The two energy transfer schemes just mentioned suggest that interesting characteristics might be expected from an energy exchange that is direct as in a jet pump, but that, at the same time, is due to the motion of pressure fields in the (stationary) frame of reference of the machine as in conventional compressors.

Such a scheme requires that the fluid of initially higher momentum takes the place of blades or pistons in conventional compressors. In analogy to other components in which a fluid medium takes over the function of solid material we shall call the devices based on these schemes "aerodynamic energy exchangers". They are the object of the investigations described in this paper.

III. The Cryptosteady Energy Exchanger

The name of this device, i.e. the term "cryptosteady", is due to Foa, who apparently was the first to report on the mode of energy exchange it utilizes 1, 2. Since this mode is not generally known, it shall be briefly described.

Suppose that a secondary fluid, which is to receive momentum from another fluid, flows steadily through an annular channel whereby the velocity vectors are parallel to the axis of the annulus. Suppose also that at same station a series of substantially axially oriented jets of another fluid (primary fluid) emerges with a steady and rather high velocity from nozzles that are evenly spaced circumferentially within the annular flow passage. If the nozzles are stationary, then one has the situation of a steady-flow ejector system with multiple driving jets. The primary fluid forms straight jets and the only transfer of mechanical energy from primary to secondary fluid is due to viscous stresses and occurs in mixing zones which grow slowly in downstream direction between the flows and eventually engulf them if the channel is long enough. Here we are interested only in the interaction over a very short distance from the merger station. Consequently we can assume that practically no mixing will occur and hence no energy is transferred from the primary fluid to the secondary fluid over the channel length of interest.

The situation changes significantly if the nozzles rotate about the channel axis. If the surrounding air would have no effect on the gas jets, they would form spiral or helical patterns even if the nozzles do not impart an angular momentum to them.

The pitch angle of these helical patterns is determined by the ratio of the circumferential velocity of the nozzles to the gas velocity at the exit sections of the nozzles. On the other hand, the paths of individual gas particles are straight and parallel to the channel axis if the gas flow has zero angular momentum. If now we consider the effect of the air on the gas jets, we observe that the gas particles will interact with air particles which, because of the helical jet patterns, stand in (the extensions of) their paths. The result is a mutual deflection of the gas jets and the air flow between them to a common direction whereby the pitch angle of the helical gas jets will be increased.

Restricting the considerations again to a short length from the merger station, we recognize that the deflected primary fluid jets look like blades of a turbo-compressor. The average pitch angle corresponds to the pitch of a row of compressor blades, and the increase of the pitch angle due to the deflection corresponds to the camber of compressor blades. Consequently, we expect that there will be a transfer of mechanical energy from the deflected gas jets ("pseude blades") to the air flow quite similar to the energy transfer from the blades of the rotor of a turbo-compressor to the medium flowing through the compressor. Like in the latter device, it involves little dissipation and it can take place over a very short distance because it is due to the glancing collision of the flows rather than the viscous entrainment of one fluid by the other.

It is obvious that the flow channel need not be formed by two co-axial cylinders. It could, in principle, be formed by various co-axial, rotationally symmetric surfaces. Depending on the geometry of the channel, one would then have situations analogous to axial, mixed-flow or radial turbomachines.

Foa has reported rather startling results for a mixed-flow arrangement of a cryptosteady energy exchanger [3]. For entrainment ratios (= ratio of secondary fluid mass flow rate to primary fluid mass flow rate) of 1 and 3 he obtained increases in stagnation pressure of the secondary fluid of more than 1000 % and 500 %, respectively, and the final stagnation pressure of the secondary fluid was, in these cases, larger than the stagnation pressure of the primary fluid at the merger station ! Even though this performance was computed by neglecting compressibility, viscosity heat conduction, and the possible desintegration of the primary fluid jets due to instabilities, we felt that a cryptosteady energy exchange mode could be of interest for hybrid propulsion systems. In fact we decided to investigate experimentally a two-stage momentum exchange scheme of which the first stage would use the cryptosteady mode while the second stage would utilize wave processes in an arrangement to be described next. A propulsion system incorporating such energy exchangers is shown schematically in Fig. 1c.

IV. The Wave Energy Exchanger

If the experience with (one-stage) axial turbo-compressors is at all relevant in the case of an axial-flow cryptosteady compressor, one expects that only a small fraction of the energy carried by the rocket gases can actually be transferred to the air. On the other hand, since piston compressors do not have the same severe limitations of the compression ratio as one-stage turbo-compressors do, it is of interest to investigate the potential of a direct energy exchange device in which the secondary fluid is acted upon in a fashion similair to that in a piston compressor.

The implementation of an energy exchange scheme, in which the primary fluid acts as pistons which compress and accelerate the secondary fluid, is, at first sight, conceptionally rather simple; One merely has to place stationary walls into the annular flow passage of the cryptosteady exchanger in such a way that the annulus is divided into a circumferential series of ducts. As they sweep across the leading edges of these walls, the fluid streams are broken up into individual packages ("charges"). In this situation, charges of primary fluid and secondary fluid enter individual ducts in sequence rather than simultaneously, provided that the width of the ducts is of the same order or smaller than the widths of individual primary and secondary fluid streams upstream of the duct entrance. Thus, the fluids have substantially the same velocity and static pressure at their contact surfaces. Moreover, even though the flow is nonsteady in the ducts, one may insure, through proper designing of the ducts, that the kinetic energies and static pressures of primary and secondary fluid, (mass-) averaged over individual charges, are nearly the same at the exit sections of the ducts.

Because the energy exchange in the ducts is, to a large extent, the result of compression and rarefaction waves, at least if the device works properly, the ducts will be called "wave tubes" and the series of ducts will be called "wave energy exchanger". It should be noted that this device is rather different from most other "wave engines' in that it does not possess flow controlling valves either at the entrance or at the exit of the wave tubes. To insure that no reverse flow or at least no appreciable reverse flow will occur, even though the wave tubes lead to a plenum chamber in which the pressure is higher than the average static pressure in front of the wave energy exchanger, it will be necessary to properly time the arrival of the primary gas jets at the entrance of the wave tubes, e.g., by judiciously selecting the rotational speed of the rotating gas divider.

Because of the very large differences in kinetic energy of primary and secondary fluid at the entrance of the wave ducts, rather large variations of pressure and velocity will occur at this position. If these variations would persist throughout the wave tubes, one would have large wall friction losses as well as a very low "effiency of non-uniformity" at the exit of the tubes. Hence any measure for the damping of the pressure and velocity fluctuations in direction of the exit sections of the

ducts is welcome. Most effective in this regard is a substantial increase of the tube cross section toward the exit. This increase has an additional advantage: As the shock, which is generated when a primary fluid column collides with a secondary fluid column, travels downstream in a duct with increasing cross section in flow direction, upstream travelling rarefaction waves are generated and these waves help to reduce the pressure build-up at the duct entrance. Thus, the danger of a sideway deflection of the primary flow jets before they have entered the wave tube may be significantly reduced.

The efficiency of the transfer of mechanical energy in the wave exchanger is expected to be substantially higher than the efficiency of an equivalent ejector, provided, of course, that most of the energy exchange is achieved by compression and rarefaction waves and weak shocks. If these waves can be generated at all, it would appear that this condition will be satisfied. Indeed, the propagation speed of energy-carrying waves is considerably larger than the transport speed of the mixing process, so that the substantially isentropic transfer of mechanical energy by the waves takes place before appreciable mixing occurs.

V. Experimental and Theoretical Investigations

The flow phenomena occuring in the aerodynamic energy exchangers being quite complex, it was decided to concentrate on an experimental investigation.

In a first step we have taken the "black box" approach, i.e., we sought some information on the overall performance of the energy exchangers without determining how this performance is actually obtained. Some analytical work was carried out in parallel, its purpose being to serve as guidance for the experimental work.

The gas generator used for our tests is a stationary rocket-type combustion chamber in which kerosene is burnt in air at pressures ranging from 8 to 15 atm., depending on the air massflow rate and fuel-air mass ratio selected. Ignition is first achieved in a pilot burner which actually is a small combustion chamber. Initial difficulties with achieving a satisfactory combustion were overcome primarily by placing a flame tube inside the cylindrical combustion chamber walls.

Typical air weight flow rates are between 1 kg/sec and 2 kg/sec. Chocked flow is achieved in the nozzles of the air feed system at all operating conditions with air manifold pressures in excess of 30 atm. These pressures and mass flow rates dictated a blow-down facility: Before each test a bank of standard high pressure bottles is filled with air up to a pressure of about 220 atm. These bottles feed the air to a heat exchanger which is designed to keep a constant temperature of the air at the manifold pressure. Typical test times are around one minute.

The only moving part of the test set-up is a rotary gas divider. This component receives the combustion gases in the form of a single flow at a static pressure equal to about 45 % of the pressure in the combustion chamber. It then devides this flow into six individual flows and expands these further. According to preliminary indications the six jets leaving the rotary gas divider were substantially overexpanded during all test runs made so far, owing in part to the fact that we had to modify the channels of the gas divider and because we have not yet operated the unit at the design conditions (stoichiometric combustion). The rotary gas divider is driven by an electric motor. Like the combustion chamber and certain other parts of the test installation it is water cooled.

So far we have tested two different configurations. The first configuration (Fig. 2) consist

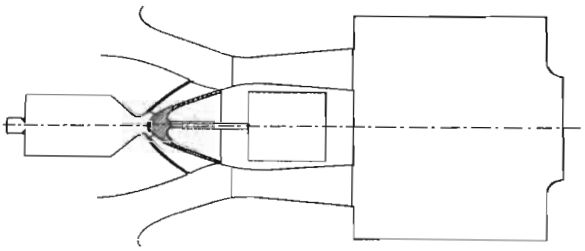

Fig. 2. Schematic drawing of experimental configuration of aerodynamic energy exchangers with gas generator and plenum chamber.

of an annular cryptosteady interaction space which, on one side, is open to the surroundings, from which air flows into it, and which admits also the six jets from the rotary gas divider. The downstream end of the cryptosteady interaction space coincides with the entrance of the wave energy exchanger. The latter is divided into a circumferential series of axially disposed wave tubes. The wave tubes are formed by plane walls which connect the inner surface of the downstream extension of the annular cryptosteady interaction space with the outer surface of this extension. The wave energy exchanger provides the only flow passages into a plenum chamber except, of course, that the latter has an opening to the surroundings. Nozzles of different sizes can be mounted in this opening, so that different compression ratios and entrainment ratios can be obtained under the same initial primary flow conditions.

The second configuration is identical with the first configuration, with the exception that the radially and axially disposed walls of the wave energy exchanger are extended in upstream direction to a position slightly upstream from the point where the primary gas jets leave the rotary gas divider and enter the annular space. Hence the second configuration does not allow any cryptosteady interaction between primary and secondary flows because the primary jets are led directly into the wave tubes.

To obtain an idea of the contribution of the cryptosteady energy exchange to the overall process, an analytical investigation of this exchange was made under some simplifying assumptions.

This analysis is presented in Appendix I.

VI. Preliminary Results

An analytical investigation of the cryptosteady energy exchange process is presented in Appendix I, Most of the many relevant parameters have been varied in a certain range. However, in Fig. 3

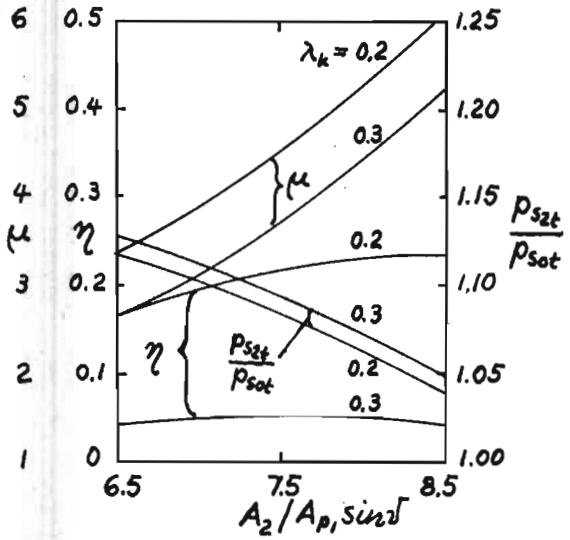

Fig. 3. Energy exchange efficiency, entrainment ratio and ratio of stagnation pressure of the air after the exchange to the initial stagnation pressure of the air for cryptosteady energy exchange with v_{pl}=2000 m/sec, $M_{pl} = 2.5$, $a_{sl_t} = a_{so_t} = 340$ m/sec, u_l = 150 m/sec, $\alpha_{pl} = \alpha_{sl} = 0^o$, $\sqrt{} = 45^o$, $A_{sl}/A_{pl} = 7.5$, $r_2/r_1 = 2.0$, $\eta_i = 0.95$, $\gamma_p = 1.25$, $\gamma_s = 1.40$.

we show only a small fraction of the numerical results. Specifically we show the energy transfer efficiency η, the entrainment ratio μ and the ratio of the stagnation pressure of the (secondary) air after the cryptosteady energy exchange to its initial stagnation pressure as a function of the ratio of flow area at the exit of the interaction space to the flow area of the primary gas at the entrance of the interaction space. Two curves are shown for each parameter. They were computed for "bulk loss factors" based on the original kinetic energy of the primary gas of 0.2 and 0.3, respectively. Other selected parameters, for the meaning of which we refer to Appendix I, are indicated in the figure caption. It can be noted that, at least under the conditions considered, no significant pumping action has been obtained. Not shown in Fig. 3 are the static pressures at the exit, which we found to be smaller or about equal to the static pressures at the entrance for the configurations investigated. The Mach numer of the primary medium decreased from its original value of 2.5 to values of about 2.3 (for λ_K = 0.2) and 2.0 (for λ_K =0.3).

The wave energy exchange being too complicated for a reasonably realistic theoretical investigation, we have concentrated on an experimental investigation. Some very preliminary results are shown in Fig. 4 together with the computed results

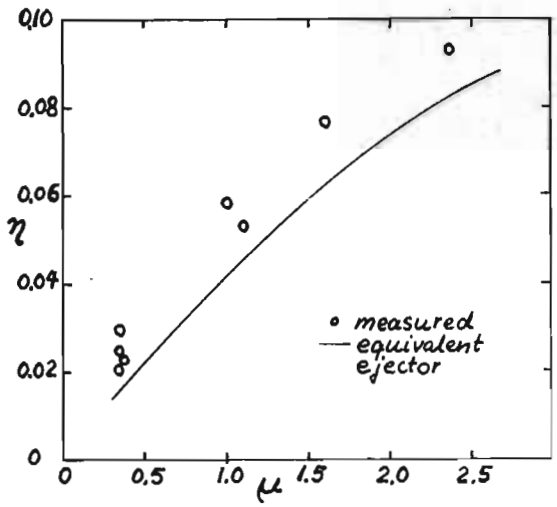

Fig. 4. Energy exchange efficiency η vs entrainment ratio μ for aerodynamic energy exchanger (experimental) and equivalent ideal ejector (calculated).

of an ideal ejector operating unter the same conditions at its merger station as our experimental device. The rather low efficiencies of the tested device and the equivalent ejector are in part due to the fact that we have not jet reached the design conditions. However, more serious is the relatively small difference in the efficiency of the aerodynamic energy exchanger and the equivalent ejector. This difference clearly points to the fact that we have not succeded, so far, to achieve proper operating conditions.

In a first attempt to find out if the low performance is due to the cryptosteady or the wave energy exchanger, we have extended the side walls of the wave tubes past the exit sections of the rotary gas divider, thus suppressing the cryptosteady energy exchange process. This change did not result in a significant change of performance, thus supporting the results of the analytical investigations, according to which no substantial cryptosteady energy exchange takes place. From pressure and temperature measurements in front of the elongated side walls of the wave tubes we have concluded that the primary gas jets do not flow correctly through the wave tubes. There seems to be a region just upstream of the wave tubes where hot primary gas lingers

practically permanently, except when we operated with the largest exhaust nozzle of the plenum chamber. This evidence motivated a brief analytical investigation of the impingement of a high-speed gas jet on an air column in a duct. The analysis for a somewhat idealized situation is presented in Appendix II. We were particularly interested in knowing under what conditions one may expect the impingement zone to move downstream into a duct. Fig. 5

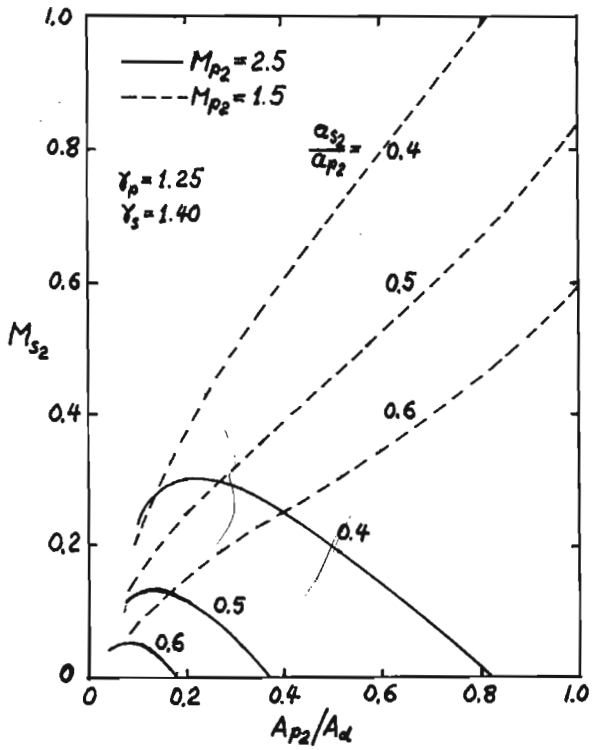

Fig. 5. Mach number of undisturbed air column in duct required for the impingement zone to remain stationary vs ratio of cross sectional area of undisturbed driving jet to cross sectional area of duct.

shows the results for the limiting case, i.e., the Mach number M_{s2} of the undisturbed air required so that the impingement zone remains stationary at the duct entrance. This Mach number is a function of the ratio of gas jet cross sectional area to the cross sectional area of the duct, of the ratio of the sonic speeds of the two fluids, and of the Mach number of the undisturbed gas jet. One may note the very large change of the required M_{s2} with a changing jet Mach number, particularly at large area ratios. Also the speed of sound ratio has a marked influence, whereby the required M_{s2} increases if the speed of sound of the gas is increased relative to that of the air. Even though we have not jet exactly measured the Mach number of the primary gas at the exit of the rotary gas divider, we have reasons to believe that it is at most 1.5. On the other hand, it is to be expected that even under proper operating conditions the secondary medium will enter a wave tube rather slowly just before the arrival of a new primary fluid jet. Hence we have tentatively concluded that we have not succeeded in moving the impingement zones downstream into the wave tubes. We believe, therefore, that a large fraction of the primary gas jets is deflected away from those wave tubes which they should enter. Thus a significant amount of primary fluid that has lost most of its originally downstream-oriented momentum flows in front of other wave tubes and must subsequently be pushed into these tubes by fresh gas jets. Moreover, the deflected primary fluid partially prevents the secondary fluid to enter the wave tubes.

The above reasoning leads us to the conclusion that a significant improvement of the performance of the wave energy exchanger can be achieved by significantly increasing the initial Mach number of the primary gas jets to values well above those which we have obtained so far, i.e., to values of 2.5 or higher.

References

1. Foa, J.V., "A New Method of Energy Exchange Between Flows and some of its Applications". Rensselear Polytechnic Inst., Dept. Aero Eng., T.R. AE 5509, Dec. 1955.

2. Foa, J.V. "Crypto-Steady Pressure Exchange". Rensselear Polytechnic Inst., Dept. Aero Eng. & Astro., T.R. AE 6202, Arch 1962

3. Foa, J.V., "A Vaneless Turbopump". AIAA Journ. 1, 466 - 467 (1963).

Appendix I: Calculation of the Cryptosteady Energy Exchange

Nomenclature:

A_{p1} = sum of the cross sectional areas of the exit slots of the rotating gas divider, measured on the surface of a cylinder with radius r_R (see Fig. 6)
A_{s1} = secondary flow cross sectional area at entrance to cryptosteady interaction space
a = speed of sound
c = relative velocity (flow velocity as seen in relative frame of reference, which rotates about the engine axis with the circumferential velocity u)
M = v/a = Mach number
$\dot{m}$ = mass flow rate
p = (static) pressure
r = distance from the engine axis
u = circumferential velocity
v = absolute velocity (flow velocity as seen in absolute frame of reference, which is stationary)
α = angle between v and meridian plane
β = angle between c and meridian plane
γ = ratio of specific heats
σ = angle between cryptosteady interaction channel and engine axis
λ_k = bulk energy dissipation coefficient
$\mu = \dot{m}_s/\dot{m}_p$ = "entrainment ratio"
η = efficiency of cryptosteady energy exchange
η_i = air intake efficiency
η_C, η_T: efficiencies of equivalent compressors and turbines
Indeces: p: primary medium (gas)
s: secondary medium (air)
t: stagnation condition
o: initial condition of fluids
1: entrance to cryptosteady interaction space
2: exit of cryptosteady interaction space

Assumptions:

1) Calorically perfect gases
2) The flows of both media are one-dimensional
3) The fraction λ_k of the initial specific kinetic energy of the primary flow and no energy of the secondary flow is dissipated during the cryptosteady interaction process
4) The dissipated energy is completely transferred from the primary medium to the secondary medium whereby no changes of the stagnation pressures result from this transfer of heat energy
5) Apart from the energy transferred according to assumption 3 no heat energy is exchanged between the flows, either through conduction, radiation or diffusion. Also, there is no viscous entrainment or mixing between the two media
6) There is no difference in static pressure of primary and secondary flow either at the entrance to or at the exit of the cryptosteady interaction space
7) While the vectors of the relative velocities of the two media have initially different directions, they are aligned at the exit of the cryptosteady interaction space just as the vectors of the relative velocities at the exit of the rotor of a turbocompressor are nearly parallel to the blade median at the trailing edge.

Initial Flow Conditions

The stagnation pressures and speeds of sound of primary and secondary flow and the Mach number of the primary flow at the entrance to the cryptosteady interaction space as well as the ratios of specific heats of the two media are assumed to be known. Hence one has

$$v_{p1} = \frac{a_{p1t} M_{p1}}{\sqrt{1 + \frac{\gamma_p - 1}{2} M_{p1}^2}} \tag{1}$$

The Mach number M_{s1} is subsonic and hence it is not known a priori. Nevertheless, we express the other secondary flow parameters in terms of M_{s1}. With $a_{s1_t} = a_{so_t}$ we get

$$v_{s1} = \frac{a_{sot} M_{s1}}{\sqrt{1 + \frac{\gamma_s - 1}{2} M_{s1}^2}} \tag{2}$$

The secondary fluid (air) is assumed to flow from the surrounding atmosphere through an air intake with known efficiency η_i to station 1. Hence we have

$$\frac{p_1}{p_{sot}} = \left(\frac{1 - \frac{1-\eta_i}{\eta_i} \frac{\gamma_s - 1}{2} M_{s1}^2}{1 + \frac{\gamma_s - 1}{2} M_{s1}^2} \right)^{\frac{\gamma_s}{\gamma_s - 1}} \tag{3}$$

and it follows for a fixed gas generator geometry that the pressure p_{pot} in the combustion chamber must be adjusted so that assumption 6, i.e., $p_{p1} = p_{s1} = p_1$ is satisfied.

The entrainment ratio is found to be

$$\mu = \frac{\gamma_s}{\gamma_p} \frac{A_{s1}}{A_{p1} \sin\sigma} \frac{a_{p1t}}{a_{sot}} \frac{\sqrt{M_{s1}^2 \left(1 + \frac{\gamma_s - 1}{2} M_{s1}^2\right)}}{\sqrt{M_{p1}^2 \left(1 + \frac{\gamma_p - 1}{2} M_{p1}^2\right)}} \frac{\cos\alpha_{s1}}{\cos\alpha_{p1}} \tag{4}$$

Velocity Triangles

The primary flow jets issuing from the slots of a rotating gas divider rotate about the engine axis with the circumferential speed u at the distance r from the axis. Hence it is useful to work not only with a stationary, absolute frame of reference but also with a relative frame of reference which rotates with the jets around the engine axis, i.e., which has the velocity u relative to the absolute frame. From geometrical considerations we have

$$c^2 = v^2 + u_1^2 \left(\frac{r}{r_1}\right)^2 + 2 v u_1 \frac{r}{r_1} \sin\alpha \tag{5}$$

and

$$v^2 = c^2 + u_1^2 \left(\frac{r}{r_1}\right)^2 - 2 c u_1 \frac{r}{r_1} \sin\beta \tag{6}$$

from which follows also

$$\sin\alpha = \frac{\frac{c}{u_1}\sin\beta - \frac{r}{r_1}}{v/u_1} \tag{7}$$

We neglect variations of the flow parameters in radial direction at each station. Because of assumption 2 we thus have only one velocity triangle for each flow at each station.

Energy Dissipation

Because of assumptions 3, 4, and 5 we can compute the change of state of the primary fluid between entrance and exit of the cryptosteady interaction region as though it would take place isentropically. Thus

$$\frac{a_{p2}^2}{a_{p1}^2} = \left(\frac{p_2}{p_1}\right)^{\frac{\gamma_p-1}{\gamma_p}} \tag{8}$$

For the secondary fluid we have

$$\frac{a_{s2}^2}{\gamma_s-1} = \frac{a_{s2}'^2}{\gamma_s-1} + \frac{\dot m_p}{\dot m_s}\lambda_k\frac{v_{p1}^2}{2} \tag{9}$$

where a'_{s2} is the speed of sound that would be reached at the exit if the change of state were isentropic. This relation can be re-written as follows

$$\frac{a_{s2}^2}{a_{s1}^2} = \left(\frac{p_2}{p_1}\right)^{\frac{\gamma_s-1}{\gamma_s}} + \lambda_k\frac{\gamma_p}{2}\frac{\gamma_s-1}{\gamma_s}\frac{A_{p1}\sin\sigma}{A_{s1}}\frac{a_{p1t}}{a_{sot}}\frac{M_{p1}^3}{M_{s1}}\frac{\sqrt{1+\frac{\gamma_s-1}{2}M_{s1}^2}}{\sqrt{1+\frac{\gamma_p-1}{2}M_{p1}^2}}\frac{\cos\alpha_{p1}}{\cos\alpha_{s1}} \tag{10}$$

Conservation Equations

The change of state of a medium in a one-dimensional flow situation usually must be computed with a system of three equations, viz. equations for the conservation of mass, momentum, and energy. In the case of two media which retain their identity in a flow process, it is necessary, therefore, to use six conservation equations. As will be seen, one must use one continuity equation and one energy equation for each of the two media and two momentum equations for the two flows combined but written for different directions.

When writing the energy equations, we make use of the fact that, in the absence of heat conduction, radiation, diffusion, and body forces, the stagnation enthalpy of fluids in steady flow can be changed only through viscous effects. We obtain particularly simple forms of the energy equation if we write the latter in the relative frame of reference, for in this frame the flows are steady and hence isoenergetic because of assumption 5, except that the energy dissipated in the primary flow must be transferred to the secondary flow (assumption 4), and the work due to the rotation of the relative frame of reference in a stationary, absolute frame must be considered because it is due to body forces.

For the primary flow we obtain

$$\frac{c_{p2}^2}{2} + \frac{a_{p2}^2}{\gamma_p-1} = \frac{c_{p1}^2}{2} + \frac{a_{p1}^2}{\gamma_p-1} - \lambda_k\frac{v_{p1}^2}{2} + L_F \tag{11}$$

where L_F is the work done by the body forces, viz. centrifugal and Coriolis forces. With

$$L_F = \frac{u_2^2}{2} - \frac{u_1^2}{2} = \frac{u_1^2}{2}\left(\frac{r_2^2}{r_1^2} - 1\right) \tag{12}$$

one gets from Eqs.(5), (8) and (11)

$$\frac{c_{p2}^2}{u_1^2} = \frac{v_{p1}^2}{u_1^2}\left[1 - \lambda_k - \frac{\left(\frac{p_2}{p_1}\right)^{\frac{\gamma_p-1}{\gamma_p}}-1}{\frac{\gamma_p-1}{2}M_{p1}^2}\right] + \frac{r_2^2}{r_1^2} + 2\frac{v_{p1}}{u_1}\sin\alpha_{p1} \tag{13}$$

and analogously for the secondary flow

$$\frac{c_{s2}^2}{u_1^2} = \frac{v_{s1}^2}{u_1^2}\left[1 - \frac{\left(\frac{p_2}{p_1}\right)^{\frac{\gamma_s-1}{\gamma_s}}-1}{\frac{\gamma_s-1}{2}M_{s1}^2}\right] + \frac{r_2^2}{r_1^2} + 2\frac{v_{s1}}{u_1}\sin\alpha_{s1} \tag{14}$$

The continuity equation for the primary medium can be written as follows:

$$\begin{aligned}\dot m_p &= A_{p1}\sin\sigma\,\rho_{p1}v_{p1}\cos\alpha_{p1}\\ &= \gamma_p p_1 A_{p1}\sin\sigma\frac{v_{p1}}{a_{p1}^2}\cos\alpha_{p1}\\ &= \gamma_p p_2 A_{p2}\frac{c_{p2}}{a_{p2}^2}\cos\beta_2\end{aligned} \tag{15}$$

where A_{p2} is that portion of the total flow cross sectional area at position 2 which is occupied by the primary fluid. From Eq.(15) it follows

$$A_{p2} = \frac{p_1}{p_2}A_{p1}\sin\sigma\frac{a_{p2}^2}{a_{p1}^2}\frac{v_{p1}}{c_{p2}}\frac{\cos\alpha_{p1}}{\cos\beta_2} \tag{16}$$

Likewise we have in the case of the secondary flow

$$A_{s_2} = \frac{p_1}{p_2} A_{s_1} \frac{\alpha_{s_2}^2}{\alpha_{s_1}^2} \frac{v_{s_1}}{c_{s_2}} \frac{\cos\alpha_{s_1}}{\cos\beta_2} \tag{17}$$

Since

$$A_2 = A_{p_2} + A_{s_2} \tag{18}$$

it follows from the last three equations

$$\cos\beta_2 = \frac{p_1}{p_2}\left(\frac{A_{p_1}\sin\sqrt{}}{A_2}\frac{\alpha_{p_2}^2}{\alpha_{p_1}^2}\frac{v_{p_1}}{c_{p_2}}\cos\alpha_{p_1} + \right.$$

$$\left. + \frac{A_{s_1}}{A_2}\frac{\alpha_{s_2}^2}{\alpha_{s_1}^2}\frac{v_{s_1}}{c_{s_2}}\cos\alpha_{s_1}\right) \tag{19}$$

This relation does not only contain the two continuity equations but also the two energy equations because of the appearance of c_{p2} and c_{s2} which are given by Eqs.(13) and (14), respectively.

In contrast to the energy, the momentum of each flow changes in all frames of reference, provided that the streamlines have different directions before and after the interaction. Because we have no a priori information concerning the momentum exchange, it is not possible to write a separate momentum equation for each flow. Instead, we must write equations for the conservation of the sum of the momenta of the two flows. However, since the momentum is a vectorial quantity, we must write these equations for more than one direction. The flows being axis-symmetric, the momentum balance must be established for the circumferential and meridian directions.

In writing the momentum equation for the circumferential direction, we have to use the moments of momentum because, in general, $r_1 \neq r_2$:

$$r_2\left(\dot{m}_p v_{p_2}\sin\alpha_{p_2} + \dot{m}_s v_{s_2}\sin\alpha_{s_2}\right) =$$

$$= r_1\left(\dot{m}_p v_{p_1}\sin\alpha_{p_1} + \dot{m}_s v_{s_1}\sin\alpha_{s_1}\right) \tag{20}$$

For the velocity triangles at position 2 we can write

$$v_2\sin\alpha_2 = c_2\sin\beta_2 - u_1\frac{r_2}{r_1} \tag{21}$$

Combining Eqs.(20) and (21) yields

$$\sin\beta_2 = \frac{\frac{r_2}{r_1} + \frac{v_{p_1}}{u_1}\frac{r_1}{r_2}\sin\alpha_{p_1} + \mu\left(\frac{r_2}{r_1} + \frac{v_{s_1}}{u_1}\frac{r_1}{r_2}\sin\alpha_{s_1}\right)}{\frac{c_{p_2}}{u_1} + \mu\frac{c_{s_2}}{u_1}} \tag{22}$$

Because of the turning of the meridian velocity components of the flows in the direction of the interaction channel (which is assumed to be straight, as shown in Fig. 6), it is rather difficult to

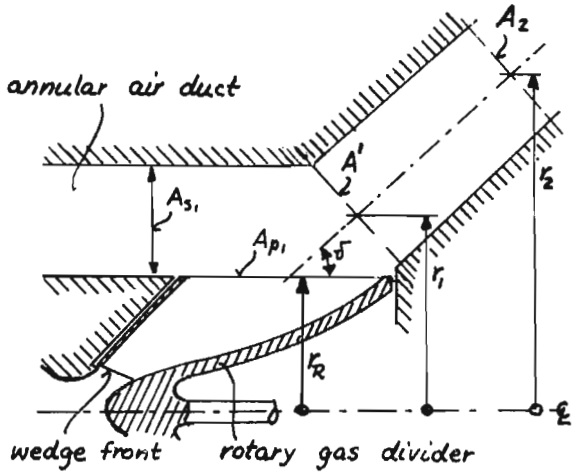

Fig. 6. Cryptosteady energy exchanger. The rotary gas divider consists of a rotationally symmetric body to which a series of wedges are attached.

write exactly the momentum equation for the meridian direction. To simplify the calculation, we compare the momentum at position 2 with the momentum at the cross section marked A' in Fig.6. Moreover, we assume that (1) the meridian velocity component of both media at this cross section points in the direction of the interaction channel, (2) no cryptosteady momentum exchange and no flow losses of any kind occur upstream of cross section A', (3) in conformance with the previously mentioned assumption (2) the pressure over the entire cross section A' is the same (and equal to p_1)*, and (4) the cross sectional area A' is equal to $A_1 = A_{p_1}\sin\sqrt{} + A_{s_1}$. Under these assumptions the momentum of the secondary fluid in meridian direction at cross section A' is very nearly the same as the original momentum $\dot{m}_s v_{s_1}\cos\alpha_{s_1}$ (in axial direction). Hence

$$\left(\dot{m}_p c_{p_2} + \dot{m}_s c_{s_2}\right)\cos\beta_2 + p_2 A_2 =$$

$$= \dot{m}_p v_{p_1}\cos\alpha_{p_1} + \dot{m}_s v_{s_1}\cos\alpha_{s_1} + p_1 A_1 + \int_{A_1}^{A_2} p\,dA \tag{23}$$

As is sometimes done in ejector calculations, we make some arbitrary assumptions concerning the pressure variation between A_1 and A_2. Already this assumption justifies, at least in part, the neglect of the actual flow phenomena upstream of cross sec-

*) Actually the pressure decreases from the inner to the outer surface of the channel as it does in a bend.

tion A' and the idealization of the flows at this cross section in accordance with the originally stated assumption (2). We assume that the pressure on the channel median varies with the square of the distance r from the engine axis, so that

$$\int_{A_1}^{A_2} p\,dA = \frac{p_2 + p_1}{2}\left(A_2 - A_1\right) - \frac{p_2 - p_1}{6}\left(A_1\frac{r_2}{r_1} - A_2\frac{r_1}{r_2}\right)\frac{\frac{r_2}{r_1} - 1}{\frac{r_2}{r_1} + 1} \qquad (24)$$

Hence we obtain from Eq.(23)

$$\cos\beta_2 = \frac{\frac{v_{p1}}{u_1}\cos\alpha_{p1} + \mu\frac{v_{s1}}{u_1}\cos\alpha_{s1}\left\{1 - \frac{\left(\frac{p_2}{p_1} - 1\right)\left(1 + \frac{A_{p1}\sin\sigma}{A_{s1}}\right)}{2\gamma_s M_{s1}^2\cos^2\alpha_{s1}}\left[\frac{A_2}{A_1} + 1 + \frac{1}{3}\left(\frac{r_2}{r_1} - \frac{A_2}{A_1}\frac{r_1}{r_2}\right)\frac{\frac{r_2}{r_1} - 1}{\frac{r_2}{r_1} + 1}\right]\right\}}{\frac{c_{p2}}{u_1} + \mu\frac{c_{s2}}{u_1}} \qquad (25)$$

Now we have reduced the problem of computing the cryptosteady interaction to a system consisting of Eqs.(18), (22) and (25) with the three unknowns β_2, M_{s1} and p_2/p_1. All other quantities appearing in these equations either are known or can be computed with the following relations: Eqs.(2), (4), (8), (10), (13) and (14). In the course of solving the above system of three equations one has to compute

$$\mu,\ \frac{a_{p2}}{a_{p1}},\ \frac{a_{s2}}{a_{s1}},\ \frac{c_{p2}}{u_1},\ \frac{c_{s2}}{u_1}.$$

After a solution has been found, one can compute v_{p2}/u_1, v_{s2}/u_1, $\sin\alpha_{p2}$ and $\sin\alpha_{s2}$ with the aid of Eqs.(6) and (7). Then one determines M_{p2} and M_{s2} and finally one can compute p_2/p_{sot} from p_2/p_1 and with Eq.(3).

It should be noted that the pressure p_2 results from the calculation if p_{sot} is specified. If both p_{sot} and p_2 were given, the problem would be indeterminate, whereby an operating condition would occur which cannot be determined with the elementary analysis of this Appendix.

Energy Exchange Efficiency

The energy exchange consists of two processes corresponding to the energy extraction from a medium in a turbine and the energy addition to a medium in a compressor. Thus the energy exchange efficiency can be thought of being composed of an equivalent turbine efficiency

$$\eta_T = \frac{h_{p1t} - h_{p2t}}{h_{p1t} - h'_{p2t}} \qquad (26)$$

and an equivalent compressor efficiency

$$\eta_C = \frac{h'_{s2t} - h_{s1t}}{h_{s2t} - h_{s1t}} \qquad (27)$$

h'_{p2t} and h'_{s2t} are the stagnation enthalpies which would be reached at station 2 if the energy exchange were isentropic.

Since no energy source or sink exists between positions 1 and 2, one has from the First Law

$$\dot{m}_p\left(h_{p1t} - h_{p2t}\right) = \dot{m}_s\left(h_{s2t} - h_{s1t}\right) \qquad (28)$$

The energy exchange efficiency η is the product of turbine and compressor efficiency. Thus, from Eqs.(26), (27) and (28) one gets

$$\eta = \eta_T\eta_C = \mu\frac{h'_{s2t} - h_{s1t}}{h_{p1t} - h'_{p2t}} \qquad (29)$$

or

$$\eta = \mu\frac{\gamma_p - 1}{\gamma_s - 1}\frac{a_{s0t}^2}{a_{p1t}^2}\frac{\frac{1 + \frac{\gamma_s - 1}{2}M_{s2}^2}{1 + \frac{\gamma_s - 1}{2}M_{s1}^2}\left(\frac{p_2'}{p_1}\right)^{\frac{\gamma_s - 1}{\gamma_s}} - 1}{1 - \frac{1 + \frac{\gamma_p - 1}{2}M_{p2}^2}{1 + \frac{\gamma_p - 1}{2}M_{p1}^2}\left(\frac{p_2}{p_1}\right)^{\frac{\gamma_p - 1}{\gamma_p}}} \qquad (30)$$

It should be noted that this efficiency would be reached only if one would succeed in separating the two media at station 2 as was suggested by Foa[3]. If the primary and secondary flows were left to flow jointly a longer distance downstream in the annulus, the kinetic energies formed with the circumferential components of the absolute primary and secondary flow velocities would be largely dissipated.

Appendix II: Calculation of the Impingement of a Gaseous Jet on a Fluid Column in a Duct

Nomenclature

A_d = duct cross sectional area
a, M, p, γ : same meaning as in Appendix I
v = flow velocity
v_I = velocity of impingement zone

v_{II} = propagation speed of shock in fluid column
ρ = density
Indeces: p, s, t: as in Appendix I
2: beginning of impingement zone
3: region between impingement zone and shock in fluid column

It is assumed that a primary fluid jet with a cross sectional area A_{p2} and an axis coinciding with the axis of a duct is directed toward the duct. Already in front of the duct the jet is embedded in a secondary flow medium that is assumed to initially have the same velocity and pressure in front of and inside of the duct. (See Fig. 7). To simplify

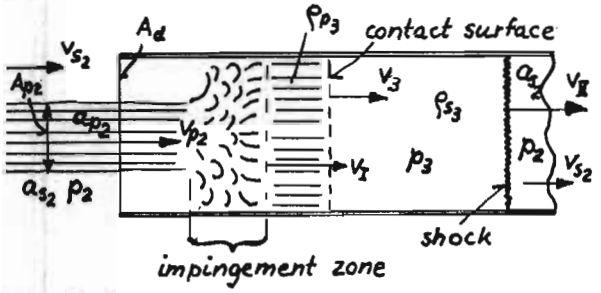

Fig. 7. The penetration of a high-velocity gas jet into a duct which is filled initially with a quiscent or slowly moving air column.

the analysis it is assumed that
(1) the duct is straight and has a constant cross section along its axis
(2) the flows are one-dimensional, except inside of the impingement zone
(3) the primary flow jet and secondary fluid are not disturbed (e.g., decelerated) upstream of the impingement zone
(4) the impingement zone has a depth which does not vary with the time
(5) the impingement zone moves downstream in the duct with a constant speed or - in the limit - is stationary and located just inside the duct
(6) no secondary fluid enters the impingement zone

It may be noted that assumptions (3) and (6) are not really compatible with each other, except when $v_{s2} = v_I$. However, since we are primarily interested in situations where these velocities are nearly equal, our assumptions lead to rather small errors.

Because of our assumption v_I = const it is appropriate to consider the changes in the impingement zone in a frame of reference which moves with this zone. The equations for the conservation of mass, momentum and energy then take on the following form:

$$A_d \rho_{p3} (v_3 - v_I) = A_{p2} \rho_{p2} (v_{p2} - v_I) \tag{1}$$

$$A_d p_3 + A_d \rho_{p3} (v_3 - v_I)^2 = A_d p_2 + A_{p2} \rho_{p2} (v_{p2} - v_I)^2 \tag{2}$$

$$\frac{(v_{p2} - v_I)^2}{2} + \frac{a_{p2}^2}{\gamma_p - 1} = \frac{(v_3 - v_I)^2}{2} + \frac{a_{p3}^2}{\gamma_p - 1} \tag{3}$$

We obtain from these equations under the assumption of a calorically perfect gas and with the relation $a^2 = \gamma p/\rho$ the following equation for the density ratio of the primary fluid:

$$\frac{\rho_{p3}}{\rho_{p2}} = \frac{1 + \gamma_p M_{p2}^2 \left(1 - \frac{v_I}{v_{p2}}\right)^2 \frac{A_{p2}}{A_d}}{2\left[1 + \frac{\gamma_p - 1}{2} M_{p2}^2 \left(1 - \frac{v_I}{v_{p2}}\right)^2\right]} + \sqrt{\frac{\left[1 + \gamma_p M_{p2}^2 \left(1 - \frac{v_I}{v_{p2}}\right)^2 \frac{A_{p2}}{A_d}\right]^2}{4\left[1 + \frac{\gamma_p - 1}{2} M_{p2}^2 \left(1 - \frac{v_I}{v_{p2}}\right)^2\right]^2} - \frac{\frac{\gamma_p + 1}{2} M_{p2}^2 \left(1 - \frac{v_I}{v_{p2}}\right)^2 \frac{A_{p2}^2}{A_d^2}}{1 + \frac{\gamma_p - 1}{2} M_{p2}^2 \left(1 - \frac{v_I}{v_{p2}}\right)^2}} \tag{4}$$

For given values of γ_p, M_{p2} and A_{p2}/A_d one can compute ρ_{p3}/ρ_{p2} as a function of v_I/v_{p2}. Also the velocity v_3 and the pressure p_3, assumed to be constant in the region between impingement zone and downstream shock in the secondary fluid column, can then be computed as a function of v_I/v_{p2}:

$$\frac{v_3}{v_{p2}} = \frac{A_{p2}}{A_d} \frac{\rho_{p2}}{\rho_{p3}} \left(1 - \frac{v_I}{v_{p2}}\right) + \frac{v_I}{v_{p2}} \tag{5}$$

and

$$\frac{p_3}{p_2} = 1 + \gamma_p M_{p2}^2 \left(1 - \frac{v_I}{v_{p2}}\right)^2 \frac{A_{p2}}{A_d} \left(1 - \frac{\rho_{p2}}{\rho_{p3}} \frac{A_{p2}}{A_d}\right) \tag{6}$$

Another dependence between v_3 and p_3 is obtained from the relations governing the changes across the normal shock in the secondary fluid column further downstream in the duct. From the well known relations

$$\frac{v_3 - v_{s2}}{a_{s2}} = \frac{2 a_{s2}}{(\gamma_s + 1) v_{II}} \left(\frac{v_{II}^2}{a_{s2}^2} - 1\right) \tag{7}$$

and

$$\frac{p_3}{p_2} = 1 + \frac{2\gamma_s}{\gamma_s + 1} \left(\frac{v_{II}^2}{a_{s2}^2} - 1\right) \tag{8}$$

one can eliminate the shock velocity v_{II} with the result

$$\frac{v_3}{v_{p2}} = \frac{v_{s2}}{v_{p2}}\left(1 + \frac{\frac{p_3}{p_2} - 1}{\gamma_s M_{s_2}\sqrt{\frac{\gamma_s+1}{2\gamma_s}\frac{p_3}{p_2} + \frac{\gamma_s-1}{2\gamma_s}}}\right) \quad (9)$$

A graphical solution is obtained by intersecting the curve v_3/v_{p2} vs p_3/p_2 obtained with Eq.(9) with a corresponding curve obtained with the aid of Eqs. (4), (5) and (6) by varying v_I/v_{p2}.